1. Mariusz MĄCZKA, 2. Stanisław PAWŁOWSKI, 3. Jolanta PLEWAKO, 4. Roman SIKORA, 5. Przemysław MARKIEWICZ

Politechnika Rzeszowska, Katedra Podstaw Elektroniki, (1),
Politechnika Rzeszowska, Zakład Elektrodynamiki i Systemów Elektromaszynowych (2),
Politechnika Rzeszowska, Katedra Energoelektroniki i Elektroenergetyki (3), Politechnika Łódzka, Instytut Elektroenergetyki (4,5),
ORCID: 0000-0003-4137-4829 (1), 0000-0003-0381-2066 (2), 0000-0002-9546-833X (3).

doi:10.15199/48.2025.01.41

Application of the boundary element method in 3D models of grounding systems

***Abstract**. The paper describes a numerical model of a grounding system enabling simulations of stationary fields in three-dimensional geometries. The developed model is based on the Boundary Element Method using the potential density function of a single layer, which makes it efficient and accurate. The results of simulations of potential distributions, electric field, and calculations of basic grounding parameters such as step voltage or ground resistance for a typical system application are presented.*

Streszczenie: W artykule opisano model numeryczny układu uziemiającego umożliwiający symulację pól stacjonarnych w geometrii trójwymiarowej. Opracowany model opiera się na Metodzie Elementów Brzegowych wykorzystując funkcję gęstości potencjału pojedynczej warstwy, co czyni go wydajnym i dokładnym. W artykule przedstawiono wyniki symulacji rozkładów potencjałów, pola elektrycznego oraz obliczeń podstawowych parametrów uziemienia, takich jak napięcie krokowe czy rezystancja uziemienia, dla typowego zastosowania systemu. (***Zastosowanie metody elementów brzegowych w modelach 3D systemów uziemień***)

Keywords: grounding system, boundary element method, step voltage, grounding resistance.
Słowa kluczowe: system uziemienia, metoda elementów brzegowych, napięcie krokowe, rezystancja uziemienia

Introduction

In the era of intensive development of technical infrastructure, ensuring the safety of people using installations or devices within its scope or directly affected by its operation plays a crucial role. There are various methods to improve safety parameters [1-2]. However, in this aspect, the key issue becomes the proper design of grounding systems, which can be implemented based on many existing and available solutions. Various available calculation methods can be used to determine the electric field distribution around the working grounding [3-9]. This makes it possible to determine the maximum values of shock voltages, which for a properly designed grounding system should not exceed the permissible values [10-14].

Figure 1 presents a model of a typical system protecting against electric shock (grounding system), along with the definition of basic parameters.

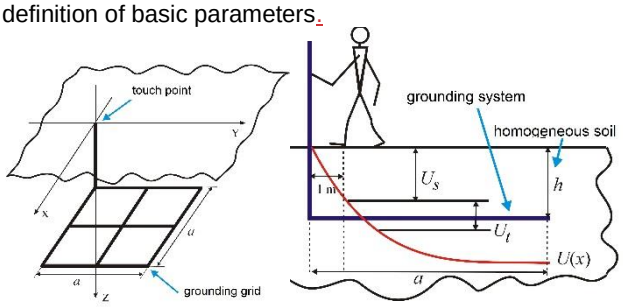

Fig. 1. Typical construction of a grounding grid: a) pictorial view of the earthing grid with a marked touch point and the geometry of the system, b) definitions of the basic system parameters,

From a technical standpoint, the design of grounding should be characterized by the lowest possible ground resistance. However, from the perspective of protection against electric shock, it must guarantee safe touch voltage (U_t) and step voltage (U_s) values for humans and animals. Precise calculation of these parameters for geometrically complex grounding structures is only possible through numerical analysis of potential distribution and current flow field. This problem can be addressed using numerical methods available within ANSYS software, as demonstrated in our previous work [15]. However, the inconveniences associated with this approach, such as the lack of access to the source code and therefore the inability to modify all, rather than just some, parameters determining the accuracy and optimization of computation time, prompted the authors to develop their own model based on the efficient Boundary Element Method (BEM) and properties of the single layer potential density function instead of using well known software used by other authors to simulation the physical phenomena such in [16].

The aim of this paper is to present a numerical model of grounding systems, enabling simulations of potential distributions and electric fields in a selected area around conducting elements constituting the planned grounding system.

The basic assumption of this model is its high efficiency and accuracy in simulating the above-mentioned parameters when defining relatively large computational areas in three geometric dimensions. As the primary means to achieve the planned objectives, the mentioned boundary element method has been selected, which restricts discretization only to the boundary of the investigated area and employs a semi-analytical approach to solving integral equations.

Numerical model

The implementation of the numerical model of the grounding system was based on the BEM, and its basic elements are illustrated in Fig 2.

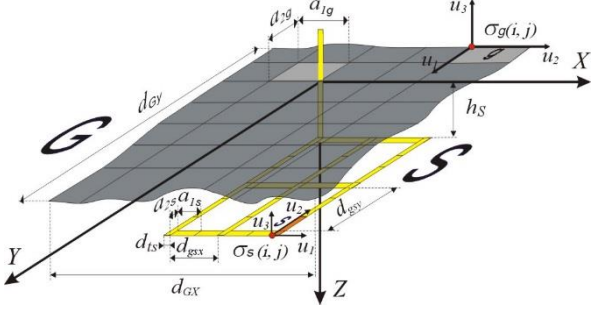

Fig 2. Numeric model of the grounding system.

Assuming that the current flow is steady-state and that the grounding structure is made of a material with

significantly higher conductivity than the ground, the problem reduces to solving Laplace's equation for the electric potential φ:

(1) $$\Delta\varphi = 0$$

with mixed boundary conditions:

(2) $$\varphi|_S = U\,, \qquad \left.\frac{\partial\varphi}{\partial n}\right|_G = 0$$

where U_p is the voltage applied to the grounding electrode, S is the surface area of the electrode, and G is the surface area of the ground. Solving this problem allows us to calculate the distribution of electric field $\vec{E}$ and current flow field $\vec{J}$ in the considered ground area according to the following relationships:

(3) $$\vec{E} = -\overrightarrow{\mathrm{grad}\varphi}, \qquad \vec{J} = \gamma\vec{E}$$

The solution to equation (1) was taken as the sum of the single layer potentials:

(4) $$\varphi(\vec{r}) = \iint_S \frac{\sigma_S(\vec{r}\,')}{|\vec{r}-\vec{r}\,'|}\mathrm{d}s + \iint_G \frac{\sigma_G(\vec{r}\,')}{|\vec{r}-\vec{r}\,'|}\mathrm{d}s$$

where σ_S, σ_G are potential density functions defined on the surfaces S and G, respectively. Regardless of the specific form of these functions, the potential defined by equation (4) exactly satisfies equation (1). Substituting (4) into the boundary conditions (2) yields a system of two integral equations for the functions σ_S, σ_G. To solve it, a rectangular discretization grid is introduced on the surfaces S and G. On each of its rectangular elements, the functions σ_S, σ_G. are approximated by step functions with respect to the variables u_1, u_2 of the local coordinate system (u_1, u_2, u_3) associated with a given grid element (see Fig 2.).

By postulating the fulfillment of the aforementioned integral equations at the midpoints of the grid elements, they are reduced to a linear system of algebraic equations in the form:

(5) $$\begin{cases} \sum_{n=1}^{N_1} \sigma_{S_{1,n}} \int_{S_{1,n}} \frac{ds_1}{|\mathbf{r}_m - \mathbf{r}|} = V_{S_1,m} & m = 1 \ldots N_S \\ \sum_{n=1}^{N_2} \sigma_{G_{1,n}} \int_{G_{2,n}} \frac{\partial}{\partial z}\frac{dg_1}{|\mathbf{r}_m - \mathbf{r}|} = 0 & m = 1 \ldots N_G \end{cases},$$

where N_S, is the number of discretization elements of the grounding grid surface, while N_G determines the quantity of discretization elements for the ground surface. The coefficients accompanying the unknowns for this system can be calculated analytically [18-19] After its numerical solution (e.g., using the Gauss method, with the selection of the maximum element), potential distributions in the specified area are calculated based on (4).

Knowledge of the potential distribution enables the direct determination of touch and step voltages. To calculate the grounding resistance R_p, it is necessary to compute the current density distribution in the ground area according to equation (3), and then the total current I flowing out of the grounding electrode:

(6) $$I = \oiint_{S'} \vec{J}\cdot\overrightarrow{\mathrm{d}s},$$

and use Ohm's law:

(7) $$R_p = \frac{U_S}{I}$$

where R_p is the ground resistance and U_S is the touch voltage.

Simulation results

Using the numerical model presented in the previous chapter, simulations of a typical grounding system described in references [15], [19] were conducted.

The basic input data of the model are contained in Table 1, where, in addition to the general geometric dimensions of the model (d_{GX}, d_{GY}), the number of grid points is provided indirectly through the number of rows in the X direction (n_{gsX},) and the number of rows in the Y direction (n_{gsX},). The table also includes information about the sizes of the discretization elements of the boundary of the simulated grounding system. Proper selection of the sizes of these elements determines, on the one hand, the accuracy of the obtained results and, on the other hand, determines the efficiency of the computations performed.

Table 1 Simulation parameters of the numeric grounding system model

Geometric dimensions of the model [m]							
d_{GX}	d_{GY}	d_{ts}	d_{gsx}	d_{gsy}	h_S	n_{gsX}	n_{gsY}
60	60	0.05	3,15	3,15	0,8	2	2
Sizes of discretization elements [m]							
a_{1g}	a_{2g}	a_{1s}	a_{2s}		U_p [V]	γ [S/m]	
0,3	0,3	0,05	0,05		240	0,01	

The parameter values in this range (a_{1g} = a_{2g} = 0.3 m and a_{1s} = a_{2s} = 0,05 m) resulted in solving the system of equations (5) of size 3870x3870, which implied a solution time of 150 s on a standard PC equipped with an i7+ processor running on Windows 11. This confirms the relatively high efficiency of the developed model.

The solution of the system of equations (5) allows for determining the potential distributions in the specified area of the model, as presented in Fig. 3

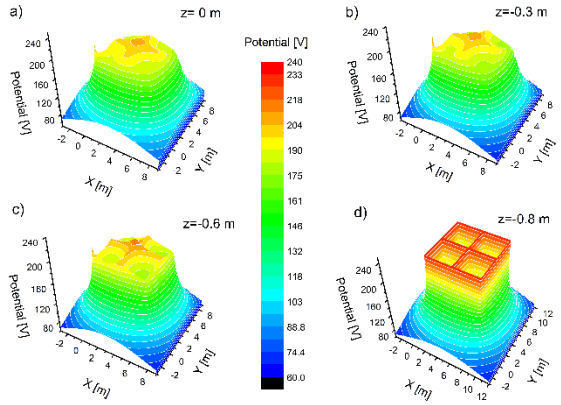

Fig. 3. Simulation results of potential distributions in the area around the grounding model defined in Table 1: a) in the plane on the ground surface and in planes at depths of 0.3 m (b), 0.6 m (c) 0.8 m (c) respectively from the ground surface

The obtained results confirmed previous calculations described in [15] which validated the correctness of the created model and allowed for further research work. As a result, additional parameters of the electrostatic field described by the equations provided in formulas (3) were determined. The simulation results in this regard are illustrated in Fig. 4, where electric field intensity distributions E are depicted in the same areas for which the results shown in Fig. 3 were plotted.

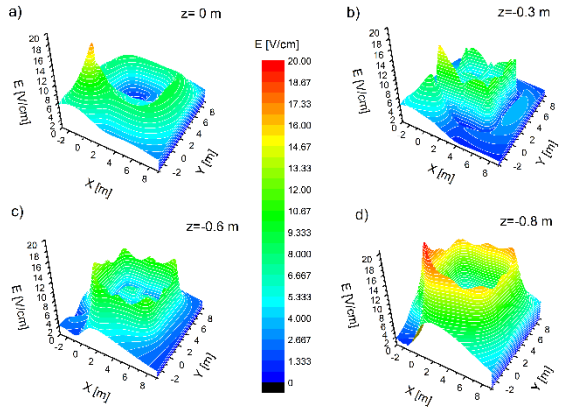

Fig. 4. Simulation results of the electric field distributions in the area around the grounding system defined in Table 1: in the plane on the ground surface (a) and in planes at depths of 0.3 m (b), 0.6 m (c), 0.8 m (c), respectively from the ground surface.

The simulations were conducted with the same resolution as the mentioned potential distributions, allowing for direct comparison and evaluation of the field effects occurring in selected areas of the model.

As could be expected, the values of electric field are strongly correlated with changes in potential, with the highest field values occurring in the vicinity of the touch point.

The grounding system parameters defined in

Fig. 1 were determined using simulations of potential distributions in the vicinity of the touch point, as illustrated in Fig. 5 and Fig. 6.

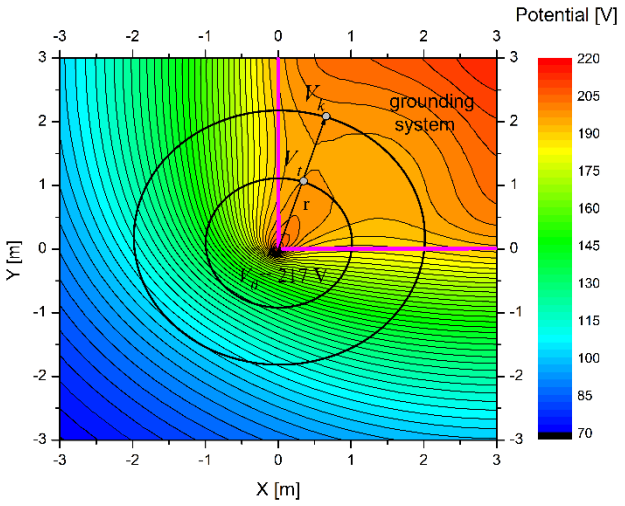

Fig. 5. Potential distribution and step voltage around the touch point of the grounding system: a) potential map with circles marking the touch (V_t) and step (V_k) potential points b) step voltage trajectories depending on the position relative to the grounding system.

The first of the above-mentioned graphs represents a map on which areas of constant potential are marked with different colors, additionally delineating contour lines. On this map, concentric circles with radii r_t = 1 m and r_s = 2 m are plotted, corresponding to the definition of touch voltage (V_t) and step voltage (V_s) respectively (see

Fig. 1). The center of both circles is located at the touch point, whose potential is denoted as V_0. For the given simulation parameters, the value of this potential at the touch point was 217 V.

Analyzing the map, it is easy to notice that the area covered by the grounding system exhibits much smaller changes in potential. To quantitatively determine these changes, touch voltages $U_t = V_0 - V_t$ and step voltages $U_s = V_0 - V_s$ were calculated (see

Fig. 1), and their changing values were plotted in Fig. 6. In part a) of this figure, changes in step voltage U_S around the touch point are illustrated along the trajectory defined by the circle with a radius r = 1 m, which is plotted in black.

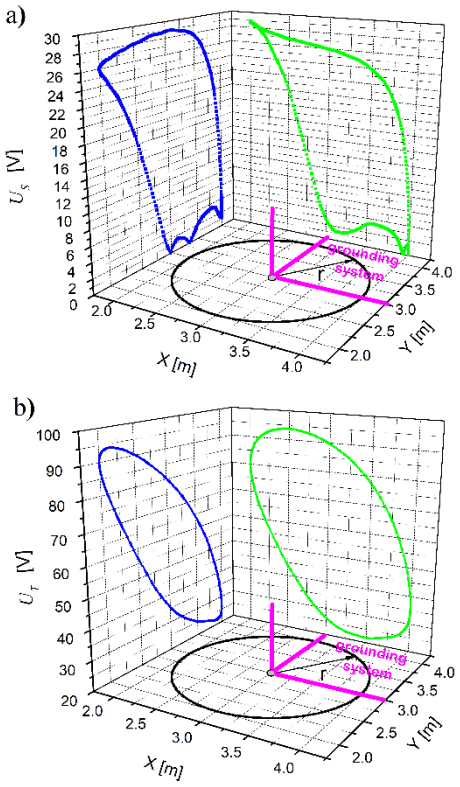

Fig. 6. Step voltage a) and touch voltage b) trajectories depending on the position relative to the grounding system.

These changes are presented as the values of U_s projected onto the XU_s plane (green points) and onto the XU_s plane (blue points). The results show that for coordinates from the first quadrant of the circle ($0 < x < 100$, $0 < y < 100$, which are within the direct influence area of the grounding system, the step voltage changes slightly (from 0 to 3.5 V). Outside the system's influence range, we observe a sharp increase in voltage, reaching levels as high as 29 V (see point x = -100, y = 100).

Changes in touch voltage U_t around the current injection point are illustrated in Fig. 6 b, where, similarly to Fig. 6 a, trajectories representing the projections of the aforementioned voltage values onto the XU_t plane (green line) and onto the YU_t plane (blue line) are plotted. As expected, the smallest voltage values occur in the first quadrant of the circle r ($0 < x < 100$, $0 < y < 100$). Using the grid of auxiliary lines, it can be read from the graph that in this area, they range from 22 V to 30 V, indicating a significant influence of the grounding system compared to values outside this area, where touch voltage values reach levels as high as 94 V.

To calculate the grounding resistance R_p, the total current I flowing in the grounding system was computed according to equation (6), reaching a value of 106 mA for the given simulation parameters. Then, using expression (7), R_p was

determined for the values of U_s provided in Fig. 6 a. The results of this operation are presented in Fig. 7, where trajectories of R_p are plotted depending on the position relative to the grounding system. The touch point was taken as the reference point, around which a circle with a radius r = 1 m was plotted, serving as guidelines for the coordinates of the points for which the value of this resistance was determined.

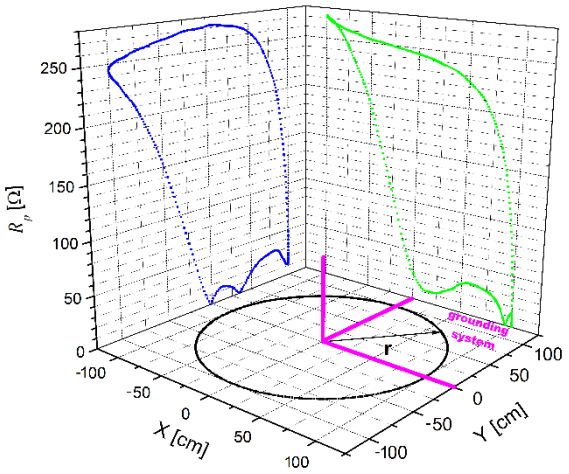

Fig. 7. Ground resistance (*R*p) trajectories depending on the position relative to the grounding system.

The simulation results are presented as values of R_p projected onto the XR_p plane (green points) and onto the YR_p plane (blue points). These results show that, as expected, for coordinates from the first quadrant of the circle (0 < x < 100, 0 < y < 100), which are within the direct influence area of the grounding system, the grounding resistance varies from a minimum value of R_p = 47 mΩ for the point at coordinates x = 94 cm and y = 34 cm to a maximum value of R_p = 32 Ω for the point at x = 59 cm and y = 81 cm. Both of these values are very small compared to those occurring outside the influence area of the grounding system, where the grounding resistance reaches a level of R_p = 272 Ω for the point at x = -100 cm and y = 6 cm.

Summary

In the study, a numerical model of the grounding system was developed, enabling simulations of stationary fields in three-dimensional geometric settings. The developed model is based on the boundary element method utilizing single-layer potential density functions, which makes it efficient and accurate.

The presented simulation results of potential distributions, electric field intensity, and calculations of basic grounding parameters such as step voltage and grounding resistance for a typical grounding system application confirm previous calculations and provide the opportunity for further research aimed at introducing innovations to enhance the safety of building users and industrial installations.

REFERENCES

[1] Otomański P., Pawłowski E. and Szlachta A. (2021) The Evaluation of Expanded Uncertainty of DC Voltages in the Presence of Electromagnetic Interferences using the LabVIEW Environment. Measurement Science Review, vol.21 (Issue 5), pp. 136-141. https://doi.org/10.2478/msr-2021-0019

[2] Pawłowski, S., Plewako, J. (2015). Applicability assessment for simplified formulas to compute surface impedance at screened surfaces. Przeglad Elektrotechniczny, 12, 182-184.

[3] Dan Y., Zhang Z., Zhao H., Li Y., Ye H., Deng J., A novel segmented sampling numerical calculation method for grounding parameters in horizontally multilayered soil, International Journal of Electrical Power & Energy Systems, vol.126, 106586, **2021**.

[4] Berberovic S., Haznadar Z., Stih Z., Method of moments in analysis of grounding systems, Engineering Analysis with Boundary Elements, vol. 27, pp. 351–360 ,**2003**.

[5] Khodra H.M., Salloumb G.A., Saraivac J.T., Matosc M.A., Design of grounding systems in substations using a mixed-integer linear programming formulation, Electric Power Systems Research, vol. 79, pp. 126–133, **2009**.

[6] Meliopoulos A.P., Feng Xia, Joy E.B., Cokkinides G.J., An advanced computer model for grounding systems analysis, IEEE Transactions on Power Delivery, vol. 8, pp.13-23,**1993**.

[7] Faleiro, G. Asensio, J. Moreno, P. Simón, G. Denche, D. García, Modelling and simulation of the grounding system of a class of power transmission line towers involving inhomogeneous conductive media, Electric Power Systems Research, vol.136, , pp. 154-162, **2016.**

[8] Faleiro E., Asensio G., Denche G., Moreno J., Electric behavior of conductor systems embedded in finite inhomogeneous volumes scattered into a multilayered soil: The problem of High-Resistivity Ratios revisited, Electric Power Systems Research, vol. 148, pp. 183–191, **2017.**

[9] Tang B., Huang Y., Liu R., Wu Z., Qu Z., Fitting algorithm of transmission tower grounding resistance in vertically layered soil models, Electric Power Systems Research, vol. 139, pp. 121–126, **2016**.

[10] Wołkowiński K.: Uziemienia urządzeń elektro-energetycznych. WNT, Warszawa, **1967**.

[11] Markiewicz H., Klajn A., Uziemienia i EMC. Układy uziomowe – Podstawowe zagadnienia konstrukcyjne. Polskie Centrum Promocji Miedzi, Wrocław, **2004**.

[12] IEEE Std 665-1995 Standard for Generating Stations Grounding, **1996**.

[13] Kostic´ V.I., Raic˘evic´ N.B., An alternative approach for touch and step voltages measurement in high-voltage substations, Electric Power Systems Research, vol.130, pp. 59–66, **2016**.

[14] Szczęsny A., Korzeniewska E.: Selection of the method for the earthing resistance measurement, Przegląd Elektrotechniczny, vol. 94, pp. 178-181, **2018,** doi:10.15199/48.2018.12.39

[15] Sikora R., Markiewicz P., Mączka M., Pawłowski S., Plewako J.: Using interpolation method to estimation step and touch voltage, Przegląd Elektrotechniczny, **2023**, vol. 2, pp. 263-266, doi:10.15199/48.2023.02.53.

[16] Lebioda, M.; Tomczyk, M. Analysis of thermal and electrical properties of heating microsystems based on TCO layers. In Proceedings of the 24th International Conference on Mixed Design of Integrated Circuits and Systems, Bydgoszcz, Poland, 22–24 June 2017; pp. 443–446.

[17] Pawłowski S.: Obliczanie pola elektromagnetycznego w transformatorach dużej mocy metodą całkowo-brzegową, praca doktorska, Instytut Elektrotechniki w Warszawie, **1993**.

[18] Mączka M., Metody efektywnego modelowania kwantowych przyrządów półprzewodnikowych, Oficyna Wydawnicza Politechniki Rzeszowskiej, **2018.**

[19] Sikora R., Markiewicz P.: Reduction of the step voltages of MV/LV substation grounding system based on shaping electric field, Archives Of Electrical Engineering, vol. 70(3), pp. 601 – 613, 2021